Oral Oncology 95 (2019) 194–201

Contents lists available at ScienceDirect

Oral Oncology

journal homepage: www.elsevier.com/locate/oraloncology

Establishment of syngeneic murine model for oral cancer therapy

Yi-Fen Chen[a], Kuo-Wei Chang[a,b], I-Ting Yang[a], Hsi-Feng Tu[b], Shu-Chun Lin[a,b,*]

[a] Institute of Oral Biology, National Yang-Ming University, Taipei, Taiwan
[b] Department of Dentistry, National Yang-Ming University, Taipei, Taiwan

ARTICLE INFO

Keywords:
Cancer
Cisplatin
Keratinocyte
microRNA
miR-134
Mouth
PD-L1
Preclinical model
Squamous
Therapy

ABSTRACT

Oral carcinoma (OSCC) is one of the most important causes of cancer death worldwide. OSCC cell lines and preclinical rodent models are crucial to addressing the mechanisms of OSCC and helping the development of new therapeutic strategies and interventions. The establishment of murine OSCC cell lines and syngeneic models are necessary to allow concordant investigation of both *in vitro* and *in vivo* pathogenesis. In this study, we established two murine tongue squamous cell carcinoma cell lines, designated MTCQ1 and MTCQ2, from 4NQO-induced OSCC using C57BL/6 mice. These cell lines express a variety of epithelial markers but produce only a tiny amount of E-cadherin. The expression of mesenchymal and stemness regulators are evident, and this is associated with the high mobility in these cell lines. MTCQ1 also shows high Ki67 and PCNA expression, and complicated alterations in *p53* expression, which may underlie its high clonogenic potential and rapid orthotopic tumor induction. Using the MTCQ1 cell subclone tagged with GFP (MTCQ1-GFP), extensive neck nodal metastasis and lung metastasis were identified by immunostaining and fluorescence imaging. Inhibition of oncogenic miRNAs, particularly *miR-134*, was able to attenuate the oncogenicity of MTCQ1-GFP. Cisplatin treatment inhibited both *in vitro* and *in vivo* growth of MTCQ1-GFP, and it was found to decrease *miR-134* expression in this subclone. The anti-PD-L1 treatment enhanced the inhibitory effects of cisplatin against tumorigenesis. This syngeneic preclinical model should help provide valuable mechanistic insights into OSCC, as well as helping with the development of new approaches to treating this disease.

Introduction

Oral squamous cell carcinoma (OSCC) is an important cause of cancer death worldwide. To elucidate the pathogenesis underlying this type of malignant transformation and to validate therapeutic strategies to treat tumor progression, the availability of preclinical models is likely to help facilitate interventions targeting this malignancy [1]. Investigations using 7, 12-dimethylbenz(a)anthracene (DMBA)-induced carcinogenesis and the hamster buccal pouch have greatly advanced our knowledge of the pathogenesis of OSCC and provided new chemopreventive insights into this disease [2–5]. 4-nitroquinoline 1-oxide (4-NQO) is a quinone-type mutagenic compound that is water soluble and causes carcinogenesis by inducing DNA adducts and double-strand break [6,7]. It is a potent carcinogen and has been shown to induce squamous cell carcinoma (SCC) in rodents, particularly tongue SCC, when administered in drinking water [8,9]. The induction of oral and esophageal SCC mediated by 4NQO has been broadly tested in various strains of rats and mice [9–12]. As C57BL/6 is the most widely used background for generating genetically modified mouse models [13], the combination of 4NQO induction with gene modification in this strain of mice has greatly helped with the mechanistic elucidation of OSCC pathogenesis [1,7,14,15]. Despite 4NQO-induced mouse OSCCs having genetic/pathological features that recapitulate human OSCC [1,11], the carcinogenic induction process is slow and takes about six months; this significantly hampers this as an approach to preclinical assessment.

Human OSCC cell lines currently available have helped bring about a greatly improved understanding of the mechanisms of OSCC oncogenesis *in vitro*. Induction of xenografic tumors in immune-incompetent mice using human OSCC cell lines allows analysis of the cell lines *in vivo* growth and metastatic potential within a 3-month period, which is far quicker than the chemical induction. However, the interaction between transplanted tumors and the tumor microenvironment can't be addressed in these immune deficient recipients [1,16]. Oral keratinocytes isolated from BALB/c mice are able to undergo transformed when treated *in vitro* with 4NQO and are able to form cell lines [17]. Two cell lines re-isolated from the allografts of immune-deficient recipients eventually were shown to display tumorigenic growth in immunocompetent syngeneic mice and this was likely to be due to the absence of CD80 (B7-1) expression [17]. Multiple cell lines have been established from DMBA-induced OSCC that has arisen in the buccal

* Corresponding author at: Institute of Oral Biology, School of Dentistry, National Yang-Ming University, No. 155, Li-Nong St., Section 2, Taipei 112, Taiwan.
E-mail address: sclin@ym.edu.tw (S.-C. Lin).

https://doi.org/10.1016/j.oraloncology.2019.06.026
Received 19 February 2019; Received in revised form 3 June 2019; Accepted 24 June 2019
Available online 28 June 2019
1368-8375/

mucosa or mouth floor of mice. The activation of the ERK-CD44 axis has been shown to determine the metastatic potential of some of these cell lines [18]. Previously we have developed a buccal pouch SCC cell line from DMBA/betel treated hamsters [5]. The efficacy and biocompatibility of nano-drugs in the abrogation of the syngeneic orthotopic growth of tumors have been validated in this preclinical model [19].

Aberrations in miRNA expression, along with dis-regulated miRNA functionality, have been shown to play pluripotent roles in OSCC pathogenesis [11,20–24]. Previously, we have determined that there is a higher susceptibility to 4NQO-induced tongue tumorigenesis in transgenic mice with *miR-31* or *miR-211* overexpression in their basal keratinocytes [7,11,14,15]. *miR-134* also drives OSCC oncogenesis by repressing a regulator that transactivates E-cadherin [22]. The oncogenic roles of *miR-21* and *miR-146a* have also been addressed in our previous studies [25–27]. Moreover, it is clear that 4NQO is able to up-regulate the expression of these oncomiRs in OSCC cell lines [11,14,21,26]. In this work, we have established two cell lines from tongue SCC tumors induced by 4NQO using C57BL/6 mice. The cell line exhibiting a more aggressive phenotype and more conspicuous genetic disruption is able to grow and metastasize in syngeneic hosts. These cell lines and their preclinical models should be a valuable approach to investigate tumor-microenvironment interactions and should also help the development of new OSCC therapeutic approaches [1,16].

Materials and methods

Induction of mouse tongue squamous cell carcinoma

To induce tongue carcinoma, 100 μg/ml of 4NQO was added to the drinking water of 6–8 week-old C57BL/6 mice (National Laboratory Animal Center, Taipei, Taiwan) for 16 weeks. The mice were then sacrificed at a time point when their body weight showed a loss of > 1/3 or at the endpoint (week 28) [11,14].

Establishment of MTCQ cell lines

Exophytic lesions on the dorsal tongue surface, size > 0.3 cm, were dissected to obtain primary cultures. The human SAS tongue SCC cell line was obtained from the JCRB cell bank. The cultivation conditions of cell lines used in this study are described in Supplementary Table S1. Defined keratinocyte serum-free medium (KSFM; Thermo Scientific, Waltham, MA) was used to limit the growth of cells other than keratinocyte. A region of the *PTGER2* gene showing high similarity between the human and mouse sequences was analyzed using species-specific PCR (Supplementary Table S2) in order to confirm the origin of all cell lines [28]. The primers used for the amplification of *p53* transcripts were listed in Supplementary Table S2. Amplicons eluted from gels were cloned into pHE vector (Biotools, Jupiter, FL), and sequenced from both directions using vector primers [29]. A stable cell subclone expressing green fluorescence protein (GFP) was achieved by selection of cells after infection with a lentivirus carrying the *GFP* gene [20]. The *miR-134*Zip viral construct has been used by us before and was described in a previous study [22]. The miRNA inhibitors are described in Supplementary Table S3. All other reagents were purchased from Sigma-Aldrich (St Louise, MO) unless it is specified otherwise.

Assays for viability, migration, invasion and colony formation

Cells were collected and seeded into 48-well plates at a density of 2500 cells per well in 4-repeats. Cell viability was analyzed over 4 days in order to generate growth curves [23]. The cell migration and invasion assays were performed using 0.8 μm 24-well Transwell chambers (Merck Millipore, Billerica, MA). For the migration assay, cells were collected and seeded into the upper surface of Transwells at a density of 1×10^5 cells per well. For invasion assay, 50 μl 10x diluted Matrigel (BD Biosciences, San Jose, CA) was used to coat the Transwell membrane. Cells were seeded onto the Matrigel-coated transwells at a density of 2×10^5 cells per well. After incubating at 37 °C for 48 h, the Transwell membranes were fixed and stained using 10 μg/ml Hoechst 33,258 for 10 min. Images of the migrated/invaded cells were captured using a fluorescence microscope [14]. The cell numbers in each picture were counted and then normalized to give fold-changes. Cells were seeded into 6-well plates at a density of 100 cells per well to allow colony formation to be assessed. Ten days later, the colonies were fixed and stained with 0.05% crystal violet. Colonies containing more than 50 cells were counted by microscopy [14].

Tumor cell transplantation

Firstly, a total of 1×10^6 cells were injected into the flank of NOD/SCID mice (National Laboratory Animal Center). These cells were 1:1 mixed with Matrigel (BD Biosciences) to give a total volume of 200 μl. The mice were sacrificed at the 5th week. Secondly, a total of 1×10^7 cells were injected into the flank of C57BL/6 mice (National Laboratory Animal Center). Cells were 1:1 mixed with Matrigel (BD Biosciences) to give a total volume of 200 μl. Mice were sacrificed at the 2nd week.

For the orthotopic isograft experiments, 5×10^6 cells in a total volume of 100 μl were injected into the central portion of the tongue of C57BL/6 mice. The mice were sacrificed between the 4th and 7th week in order to assess the growth of the primary tumor and determine the presence of neck metastasis. For the regional metastasis assay, 5×10^6 of cells (in 100 μl volume) were injected into the central portion of the tongue of nude mice (National Laboratory Animal Center). The mice were sacrificed at the 3.5th weeks and the tongue tumors and neck tissues were then isolated for histopathological and immunohistochemistry (IHC) evaluation. For the distant metastasis assay, 1×10^6 cells were injected intravenously into C57BL/6 mice. Mice were sacrificed when their body weight loss was > 1/3 or at the 7th week. Autopsies were performed to evaluate the presence of metastatic tumor foci in their various organs.

To test the therapeutic efficacy of cisplatin (CDDP) and anti-PD (CD1)-L1 antibody, cells were mixed 2:1 with Matrigel (BD Biosciences) to give a total volume of 150 μl, which was then injected into C57BL/6 mice subcutaneously. At the 2nd or 3rd week after tumor injection, 2 or 6 mg/kg of CDDP dissolved in 0.9% saline was intraperitoneally injected every other day for 2 to 4 weeks, while the control group received an injection of an equal volume of 0.9% saline [30]. Mouse anti-PD-L1 (clone 10F.9G2) and its isotype control antibody (IgG2b clone LTF-2) were purchased from BioXCell (Lebanon, NH). At the 2nd week after tumor injection, mice were injected every other day intraperitoneally with 200 μg antibodies in PBS per dose until the end point [31]. The visualization, measurement and processing of tumors followed the protocols we previously established [14,29]. All animal studies were carried out in accordance with the guidelines of the National Yang-Ming University Institutional Animal Care and Use Committee (IACUC).

Statistical analyses

All data are presented as means ± SE. Mann-Whitney tests, *t*-tests, and two-way ANOVA tests were used to compare the differences among the various subsets. A *p*-value less than 0.05 was considered statistically significant. *ns*, not significant; *, $p < 0.05$; **, $p < 0.01$; ***, $p < 0.001$.

Results

Establishing and characterizing the cell lines

Upon sacrifice of the mice, tumors on the dorsal surface of the resected tongues were dissected out (Fig. 1A). The main section of each tumor mass was washed, minced up and then digested with dispase in

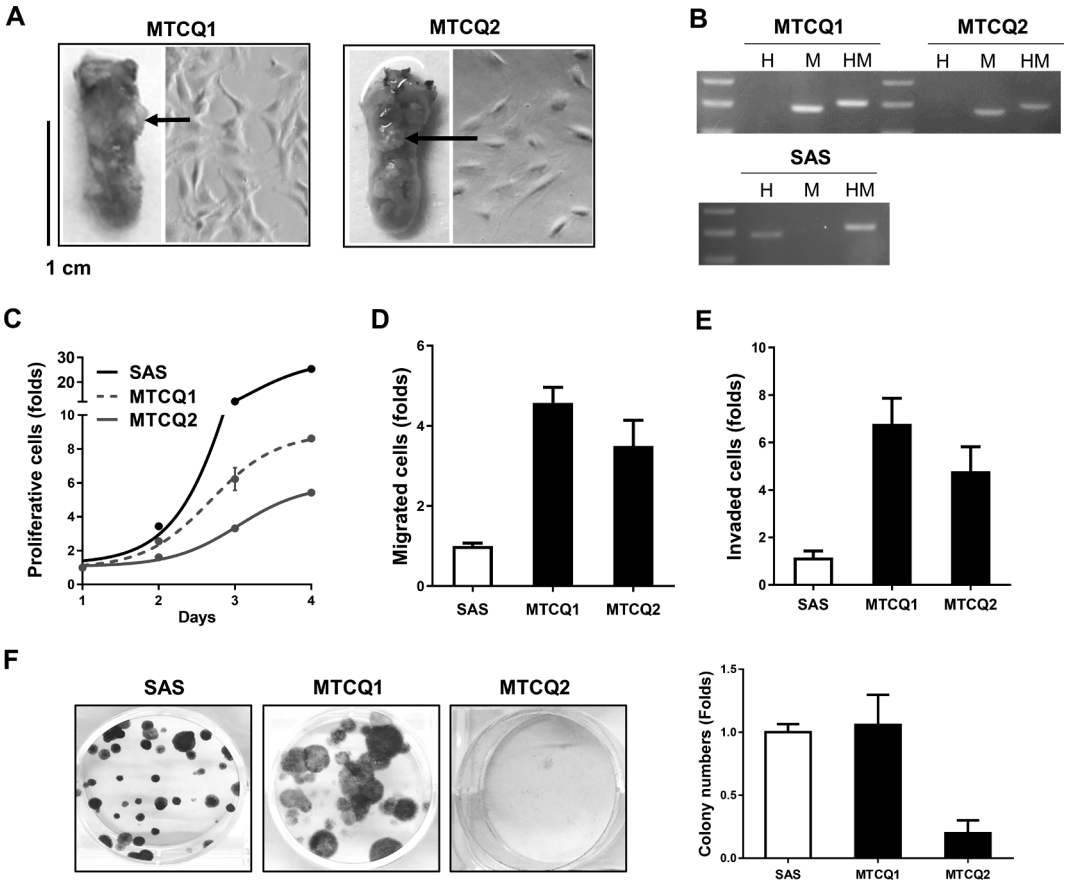

Fig. 1. Establishment of the cell lines and their phenotypic characterization. (A) Resected tongues (Lt) and the morphology of the MTCQ1 and MTCQ2 cell lines were established using tumors (Rt, X200). The arrows indicate the tumors used for establishing the cell lines. (B) Typing of cell origin of the cell lines using PCR analysis. H, human; M, mouse; HM, both human and mouse. The results show that these cell lines originate from mouse. Neg, negative control. The other lanes in the gels are molecular weight markers. (C - E) Quantification of proliferation, migration, and invasion relative to the SAS cell line. (F) Colony formation capability. Left, images of representative culture dishes. Right, quantification.

order to release the tumor cells. The remained tissue was embedded to allow histopathological evaluation in order to confirm malignancy. The dissociated cells were cultivated in 10% DMEM for two weeks to allow population expansion to occur, and then the cells were cultivated in KSFM for three weeks to eliminate any contaminating mesenchymal cells. Two individual primary cell lines were obtained that showed continuous growth for more than 20 weeks and these were designated as the mouse tongue carcinoma, 4NQO induced (MTCQ) series, namely MTCQ1 and MTCQ2. The cells forming these cell lines exhibit polygonal, ovoid or spindle shapes (Fig. 1A). PCR genotyping validated the fact that they had originated from mouse (Fig. 1B). The MTCQ cells had lower proliferation capability compared to SAS cell, however, MTCQ1 proliferated more rapidly than MTCQ2 (Fig. 1C). Furthermore, the abilities of the MTCQ cell lines in migration and invasion were much higher than SAS cell (Fig. 1D, E). MTCQ1 exhibited a potent ability to form colonies, which is similar to the SAS cell (Fig. 1F). By way of contrast, the ability of MTCQ2 to form colonies was nearly absent. Finally, the colonies formed by MTCQ1 were much bigger than those formed by the SAS cell.

Gene expression profiling

The expression of Ki67 and PCNA in the MTCQ1 cell was higher than that in the MTCQ2 cell. Both MTCQ cell lines expressed a range of keratinocyte markers with the exception that only scanty levels of E-cadherin were expressed in both lines. Both cell lines also expressed various mesenchymal markers, such as vimentin, fibronectin, ZEB1, SMA and other proteins, as well as PD-L1, CD80, p16 and Ras variants (Fig. 2A). The expression of stemness markers in MTCQ1 was stronger than in MTCQ2. MTCQ1 expressed intense p53 protein with a smaller molecular weight (Fig. 2A). RT-PCR analysis revealed the truncation of exon 8-11 sequences for about 100-bp in the *p53* transcript of MTCQ1 cell (Fig. 2B). Sequencing analysis revealed that the MTCQ2 cell expressed a wild type *p53* gene sequence. On the other hand, an analysis of MTCQ1 showed the presence of a GTG to TTG mutation causing a V214L change in the *p53* gene of this cell line, which corresponds to a V211L change in the human *p53* gene. The *p53* gene sequence in MTCQ1 also was truncation from codon 329 to codon 391, and this region of the protein was replaced by 13 aberrant amino acid residues that stretched from codon 329 to codon 341 (Fig. 2C). The whole exon sequencing confirmed the presence of *p53* alterations in MTCQ1 genome. However, no *p16* or *Ras* gene mutation was found in MTCQ cells.

We generated a MTCQ1-GFP cell subclone for the subsequent experiments. Green fluorescence was able to be readily discerned in this cell subclone (Fig. 3A). Comparing to MTCQ2, MTCQ1 is less sensitive to cisplatin (CDDP). Nonetheless, the MTCQ1-GFP cell subclone had the same CDDP sensitivity as the parental MTCQ1 cell (Fig. 3B). It was intriguing to note that there was a re-appearance of significant E-cadherin expression and a decrease in Snail, p53 and SOX2 expression when the MTCQ1-GFP cell subclone was treated with CDDP (Fig. 3C). The CDDP treatment also suppressed *miR-134* expression in the MTCQ1-GFP cell subclone (Fig. 3D).

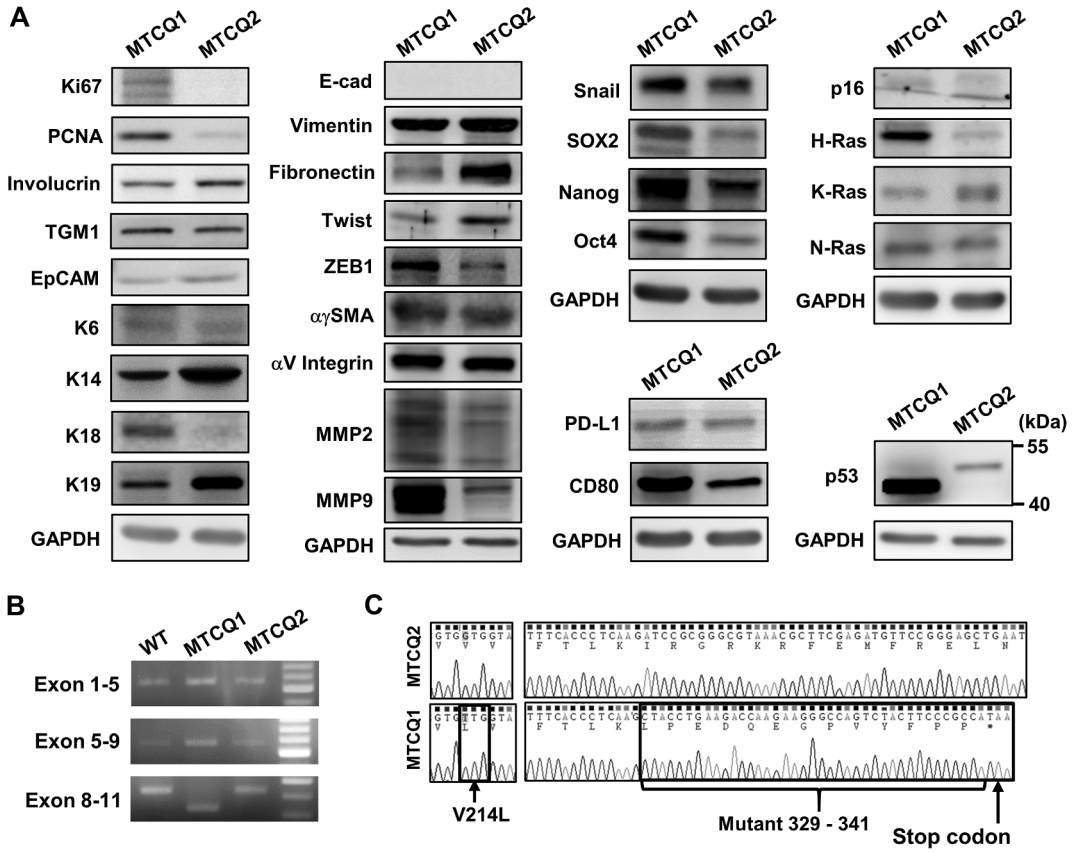

Fig. 2. Analysis of gene expression and *p53* mutation. (A) Western blot analysis of gene expression. Left, proliferation and differentiation genes; Left Middle, EMT-associated genes; Middle Right, stemness and immune-escape regulators; Right, p16, Ras and p53. The size of molecular weight markers is provided in p53 analysis panel. (B) Amplification of *p53* transcript using RT-PCR analysis. The right most lanes are molecular weight markers of 100-bp ladder. The strongest bands designate 500-bp position. (C) *p53* sequencing. The results reveal the presence of a missense mutation, gene truncation and sequence disruption within the *p53* gene of MTCQ1. Short arrow, the mutated nucleotide; Long arrow, stop codon.

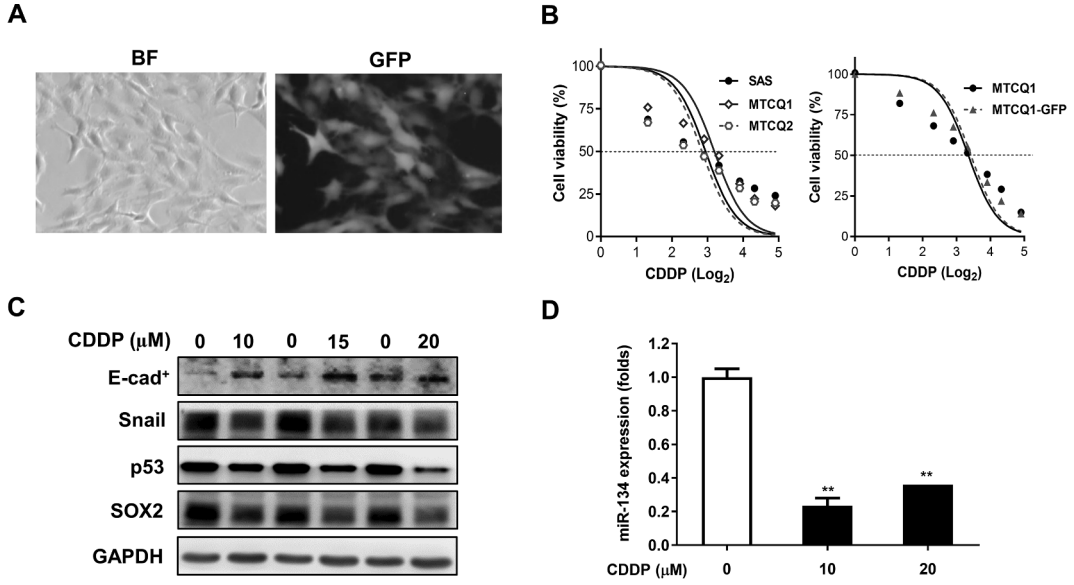

Fig. 3. Establishment and characterization of MTCQ1-GFP cell subclone. (A) Cell morphology of the MTCQ1-GFP cell subclone. X100. Left, bright field (BF) photography. Right, green fluorescence (GFP) photography. (B) Dose-response curves of the cells following CDDP treatment for 24 h. Left, MTCQ1, MTCQ2 and SAS cells. Right, MTCQ1 and MTCQ1-GFP cells. (C) Western blot analysis comparing the expression levels of E-cad, Snail, p53 and SOX2 in the MTCQ1-GFP cell subclone before and after the treatment with various doses of CDDP. (D) qRT-PCR analysis to detect *miR-134* expression in the MTCQ1-GFP cell subclone following CDDP treatment. $^{+}$, prolonged exposure of image.

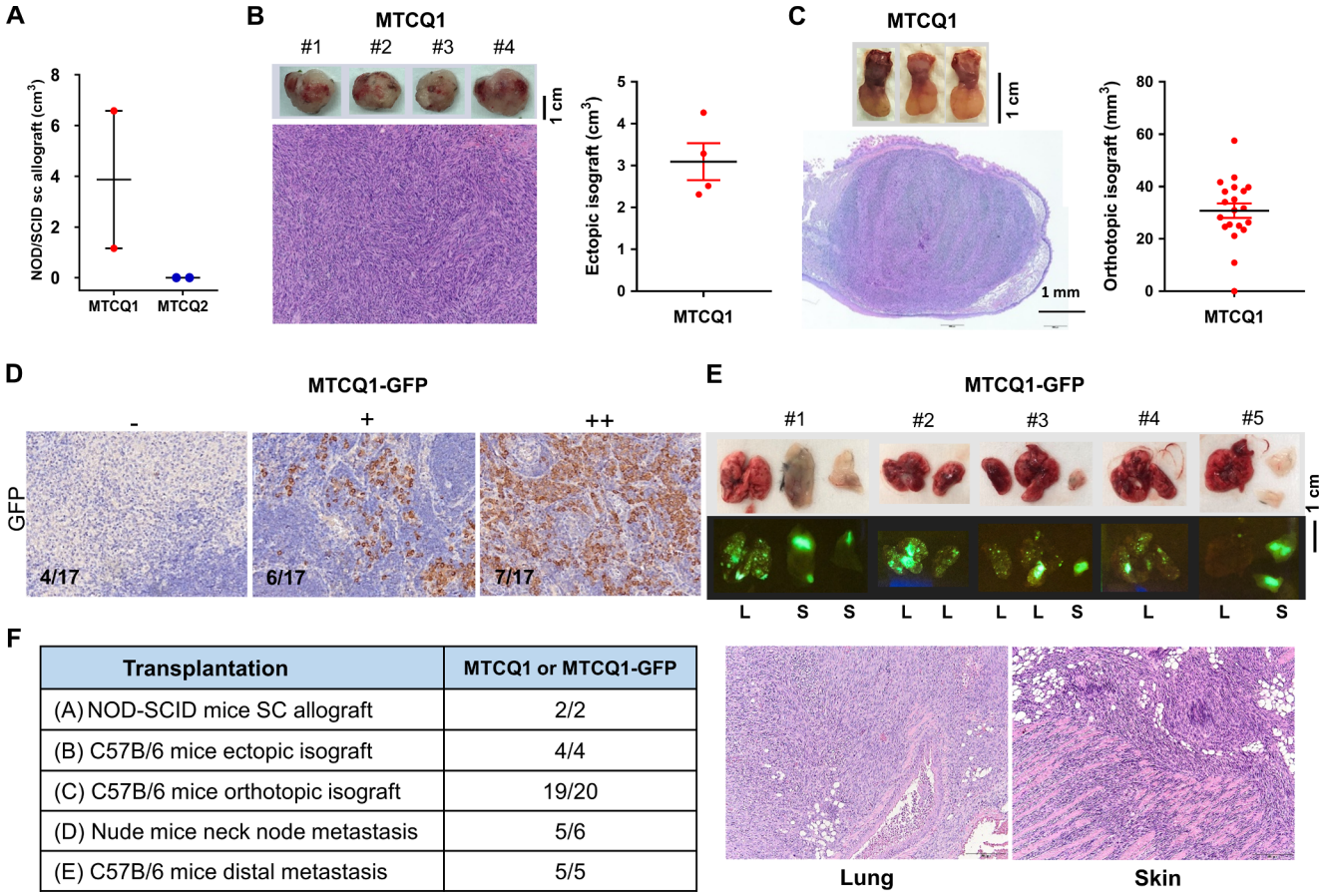

Transplantation	MTCQ1 or MTCQ1-GFP
(A) NOD-SCID mice SC allograft	2/2
(B) C57B/6 mice ectopic isograft	4/4
(C) C57B/6 mice orthotopic isograft	19/20
(D) Nude mice neck node metastasis	5/6
(E) C57B/6 mice distal metastasis	5/5

Fig. 4. Transplantation of the MTCQ1 cell line. (A) Subcutaneous allografic induction of the two cell lines admixed with Matrigel using NOD-SCID mice. Only MTCQ1 is tumorigenic. (B) Subcutaneous isografic induction of cells in C57BL/6 mice. Left Upper, gross pictures of tumors; Left Lower, a representative histopathological picture. X100. Note the high cellularity in tumor tissue. Right, quantification of tumor size. (C) Orthotopic isografic induction of MTCQ1 in C57BL/6 mice. Left Upper, representative gross picture of tongues; Left Lower, a representative histopathological section of a tongue. X50. This reveals the presence of the tumor in the tongue. Right, quantification of the size of orthotopic isografts. (D) Immunohistochemistry based on GFP within the neck lymph nodes of nude mice that had received orthotopic MTCQ1-GFP allografts. X50. −, negative, +, weak positive; ++, strong positive. (E) Tail vein injection of MTCQ1-GFP into C57BL/6 mice. Upper, Gross pictures; Middle, fluorescence images. L, lung; S, skin. Note the metastatic fluorescent nodules that are present in these tissues. Lower, histopathological sections of lung and skin revealing the involvement of metastatic cells. (F) A summary of the transplantation assays performed during this study.

Tumor cell transplantation

We first performed allotransplantation of cell lines admixed with Matrigel into the flank of NOD/SCID mice. Over a five-week-period, mice that had received MTCQ1 cell injection showed growth of a tumor, but, on the other hand, the mice that had received the injection of MTCQ2 cell did not exhibit any growth of tumors (Fig. 4A). The cells in MTCQ1 graft were re-cultivated for subsequent experiments. The subcutaneous tumorigenicity of the MTCQ1/Matrigel cells in syngeneic mice was potent and consistent (Fig. 4B). Orthotopic MTCQ1 isografts were induced in nearly all hosted syngeneic mice (Fig. 4C). To confirm that the MTCQ1 cell subclone is capable of forming neck metastasis, orthotopic allograft of the MTCQ1-GFP cell subclone into the tongue was carried out in nude mice. An IHC analysis of the dissected neck tissues from these mice revealed the presence of GFP-positive cells in more than 76% (13/17) of their lymph nodes (Fig. 4D). The MTCQ1-GFP cell subclone was also injected into the tail vein of syngeneic mice to determine whether it had the potential to bring about distal metastasis. Over the follow-up period for 7 weeks, all of the injected mice were found to have diffused or scattered fluorescent nodules in the lungs and in the skin (Fig. 4E). Histopathological examination of the animals confirmed the existence of metastatic lesions in their lung and skin tissue. Fig. 4F elaborates on the ability of MTCQ1 to induce primary tumors, regional metastasis, and distal metastasis.

Inhibition of oncomiRs reduced MTCQ1-GFP oncogenicity

The MTCQ1-GFP cell subclone was treated with inhibitors targeting *miR-21*, *miR-31*, *miR-134*, *miR-146a* and *miR-211*, which are 4NQO-inducible oncomiRs [11,14,21,26], in order to address if these oncomiRs are involved in pathogenesis. Except for the *miR-211* inhibitor, these inhibitors were able to clearly reduce the endogenous expression of these oncomiRs in a significant manner (Fig. 5A). Treatments with the inhibitors targeting *miR-21*, *miR-134* and *miR-211* were able to reduce the growth of cells. The inhibition of *miR-134* yielded the most significant effect (Fig. 5B). Treatment with all of these oncomiR inhibitors was able to significantly sensitize the cell to CDDP. Inhibition of *miR-134* yielded the greatest effect again (Fig. 5C). Treatment with all of these inhibitors was able to attenuate migration and invasion, abet to different extents (Fig. 5D, E). *miR-134* inhibition also resulted in the greatest attenuation in migration and invasion. Combined treatment with the inhibitors of *miR-31* and *miR-146a* resulted in more profound inhibition of migration than either of these two inhibitors alone. However, the addition of either *miR-31* inhibitor or *miR-146a* inhibitor to *miR-134* inhibitor did not result in any synergic effect regarding cell migration (Fig. 5F). To confirm the efficacy of *miR-134* inhibition in oncogenic abrogation, MTCQ1-GFP cell subclone was infected with a lentivirus carrying *miR-134*Zip [22]. The inhibition brought about by the Zip construct was found to decrease oncogenicity and increase the

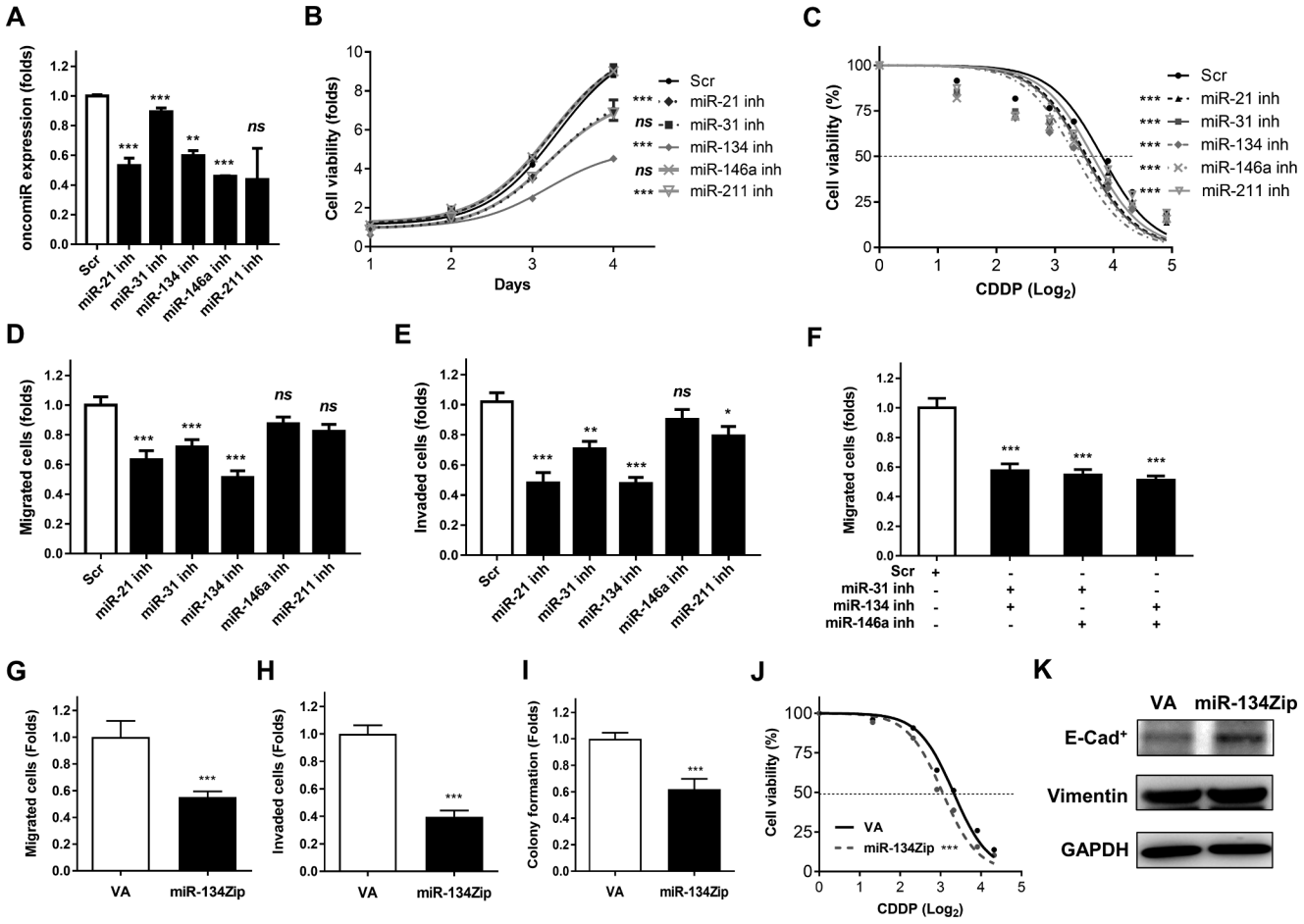

Fig. 5. Inhibition of oncomiRs using the MTCQ1-GFP cell subclone. (A) qRT-PCR analysis. The results reveal that there is a decrease in expression of the oncomiRs following the treatment with the relevant inhibitors. (B – E) Cell proliferation, the responses to CDDP treatment in terms of migration and invasion assays. The results reveal an association between oncomiR inhibition and an attenuation of the tumor phenotypes. (F) Migration. Combined inhibition using oncomiRs is unable to bring about a further additive effect regarding cell migration. (G - J). Delivery of *miR-134*Zip inhibits cell proliferation, migration and invasion, and increases CDDP sensitivity. (K) Western blot analysis reveals that there is increased E-cad expression, without any change of vimentin expression following *miR-134* inhibition. $^{+}$, prolonged exposure of image. inh, inhibitor.

sensitivity of MTCQ1-GFP cell subclone to CDDP (Fig. 5G-J). *miR-134* inhibition also resulted in an increase of E-cadherin expression in this cell subclone (Fig. 4K). Based on the above, it seems likely that the 4NQO modulated oncomiRs, particularly *miR-134*, contribute to varying degrees to the neoplastic pathogenesis of MTCQ1 cell line.

CDDP and anti-PD-L1 inhibit MTCQ1 tumorigenesis

To assess the ability of CDDP in abrogating the tumorigenesis, subcutaneous injection of MTCQ1 cells or MTCQ1-GFP cells, admixed with Matrigel, was carried out using syngeneic mice. These mice then received 2 mg/kg intraperitoneal CDDP treatment every other day starting from the 2nd week. CDDP treatment significantly retarded the growth of tumors caused by these two cell lines (Fig. 6A), and resulted in a reduced tumor weight relative to the control tumors (Fig. 6B - D). CDDP treatment significantly decreased the *miR-134* expression in tumors (Fig. 6E). Anti-PD-L1 treatment did not cause tumor inhibition in the first two weeks. But the treatment retarded the tumor growth in the subsequent two weeks (Fig. 6F). Furthermore, the combined regiment of CDDP and PD-L1 blockage conferred the most remarkable tumor inhibition (Fig. 6F – H).

Discussion

The cells obtained from 4NQO induced tongue SCC exhibit molecular and pathological changes that resemble those that occur in their human OSCC counterparts [1,32]. To generate cell lines from such malignancies will help significantly by providing functional insight into OSCC pathogenesis. In addition, isografic growth of tumor cells in a syngeneic mouse should also help with the analysis of the interplay between tumors and immune responses. The C57BL/6 strain is the main mouse background used for genetic modification [13]. Here we report that two cell lines, MTCQ1 and MTCQ2, have been established from tongue SCC after 4NQO treatment of C57BL/6 mice. In addition to its ability to be cultivated *in vitro*, MTCQ1 also grows and metastasizes when transplanted into syngeneic mice. This implies that the cell and animal models described in this work will in the future be useful platforms when assaying the progression of OSCC and exploring new therapies to treat OSCC.

Both the MTCQ1 and MTCQ2 cell lines express a range of squamous markers to a significant level, nevertheless they only express a very small amount of E-cadherin. Furthermore, both cell lines also express various mesenchymal markers, in particular vimentin. A decrease in or the silencing of E-cadherin expression, and/or the gain of epithelial-mesenchymal transition (EMT) characteristics are critical events in OSCC progression [22]. We have recently identified that *miR-134* up-regulation is likely to underlie the E-cadherin down-regulation found in human OSCC [22]. This study further confirms the CDDP treatment represses *miR-134* expression and restores some E-cadherin expression in the MTCQ1-GFP cell subclone. In addition, *miR-134* inhibition also

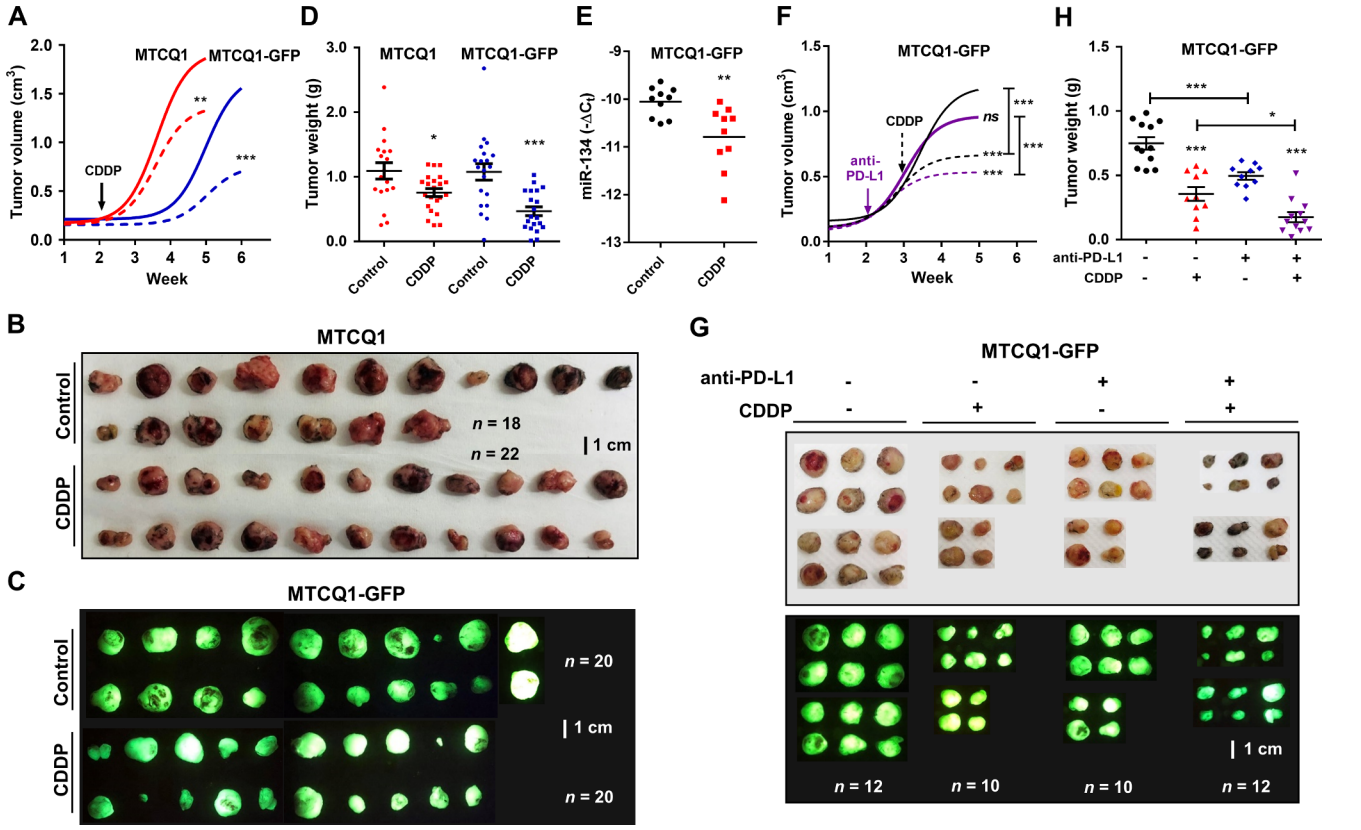

Fig. 6. CDDP and anti-PD-L1 treatments inhibit the growth of MTCQ1 isografts. (A) Growth curve of MTCQ1 and MTCQ1-GFP isografts. Solid lines, CDDP treatment; Dot lines, saline injection. Red, MTCQ1 cells; 10^7 cell inoculation; Blue, MTCQ1-GFP subclone cells; 5×10^6 cell inoculation. Arrow, start point of 2 mg/kg CDDP or control injection. (B, C) The resected MTCQ1 and the MTCQ1-GFP isografts tumors harvested at the end points. (B) Bright light image; (C) Fluorescent image. (D) Quantification of tumor weight. CDDP treatment significantly decreases the weight of isografts. Red, MTCQ1 cell; Blue, MTCQ1-GFP cell subclone. (E) *miR-134* expression. The results show decreased *miR-134* expression in the CDDP treated MTCQ1-GFP tumors relative to the control tumors. The control tumors are tumors numbers 1, 2, 5, 6, 9–11, 13, 16 and 20, which weight 1.28 ± 0.01 g. The CDDP-treated tumors are tumors numbers 4, 5, 7, 8, 11, 13, 15, 16, 19 and 20, which weight 0.46 ± 0.08 g. (F) Growth curve of MTCQ1-GFP isografts following injection of 5 x10^6 cells. Arrows, start points of anti-PD-L1 antibody, 6 mg/kg CDDP or control injection. Black solid line, control; Purple solid line, anti-PD-L1 treatment; Black dot line, CDDP treatment. Purple dot line, combined anti-PD-L1 and CDDP treatments. (G) The resected MTCQ1-GFP isografic tumors harvested at the end points. Upper, Bright light image; Lower, Fluorescent image. (H) Quantification of tumor weight. Combined anti-PD-L1 and CDDP treatments significantly decrease the growth of MTCQ1-GFP isografts comparing to solitary treatment.

increases E-cadherin expression in this subclone. Since the blockage of *miR-134* results in a potent inhibition of MTCQ1-GFP growth and aggressiveness, this cell model may capture various key features of human oral carcinogenesis. Although the validity and efficacy of miRNA inhibitors and Zip experiments with regard to their effect on tumorigenesis need further elucidation, this study pinpoints clearly the potential of these molecules in attenuating the oncogenicity of a murine OSCC cell line.

MTCQ1 exhibits more aggressive behaviors than MTCQ2. The higher expression of proliferative and stemness markers, as well as the presence of a mutation in *p53*, both of which are found with MTCQ1 and not with MTCQ2, seem to be correlated with the above specific phenotypes. This aggressiveness, along with the various complicated molecular disruption, may be responsible for the ability to undergo subcutaneous growth, to promote orthotopic growth, to bring about the regional neck dissemination and to allow distal metastasis in the host mice. The neck node metastasis and lung metastasis brought about by the MTCQ1-GFP cell subclone are readily identifiable by immunostaining or fluorescence detection, and therefore would be contributive to identifying factors involved in tumor spread. We also validate the efficacy of tumor ablation by various oncomiR inhibitors and this further substantiates the contribution that these oncogenic miRNAs make regarding murine tumorigenesis; these findings agree with the findings for human OSCC [7,14,15,20–22,25,27].

To eliminate tumor stemness seems to be one of the more useful strategies available when treating cancer [33]. Although, we are unable to address how the expression of p53, SOX2 and snail are down-regulated following cisplatin treatment *in vitro, miR-134* inhibition does enhance the effects of cisplatin in terms of modulating gene expression and bring about tumor inhibition. Thus, our animal model should be further applicable when investigating neoplastic processes involving EMT and stemness and when trying to improve a given therapeutic regimen. In summary, this study has developed two murine tongue SCC cell lines. Although we have demonstrated the efficacy of CDDP and PD-L1 blockage in abrogating the tumor growth *in vivo* [31], future studies using these lines, together with the validation of their linked clinical models, should provide valuable information and help greatly our understanding of the interactions between OSCC and its microenvironment. Furthermore, they should be able to help test the validity of anti-OSCC immune therapies when treating OSCC [16].

Declaration of Competing Interest

The authors declare no conflict of interest.

Acknowledgments

This study was supported by grants MOST102-2628-B-010-006-MY3

and MOST105-2314-B-010-027-MY3 and Postdoc Research Grants MOST105-2811-B-010-041, MOST106-2811-B-010-036, and MOST107-2811-B-010-520 for Dr. Yi-Fen Chen from the Ministry of Science and Technology, Taiwan.

Appendix A. Supplementary material

Supplementary data to this article can be found online at https://doi.org/10.1016/j.oraloncology.2019.06.026.

References

[1] Ishida K, Tomita H, Nakashima T, Hirata A, Tanaka T, Shibata T, et al. Current mouse models of oral squamous cell carcinoma: Genetic and chemically induced models. Oral Oncol 2017;73:16–20.
[2] Silberman S, Shklar G. The effect of a carcinogen (Dmba) applied to the hamster's buccal pouch in combination with croton oil. Oral Surg Oral Med Oral Pathol 1963;16:1344–55.
[3] Kowshik J, Mishra R, Sophia J, Rautray S, Anbarasu K, Reddy GD, et al. Nimbolide upregulates RECK by targeting miR-21 and HIF-1alpha in cell lines and in a hamster oral carcinogenesis model. Sci Rep 2017;7:2045.
[4] Chang KW, Lin SC, Koos S, Pather K, Solt D. p53 and Ha-ras mutations in chemically induced hamster buccal pouch carcinomas. Carcinogenesis 1996;17:595–600.
[5] Lin SC, Chang KW, Chang CS, Yu SY, Chao SY, Wong YK. Establishment and characterization of a cell line (HCDB-1) derived from a hamster buccal pouch carcinoma induced by DMBA and Taiwanese betel quid extract. Proc Natl Sci Counc Repub China B 2000;24:129–35.
[6] Gunji A, Uemura A, Tsutsumi M, Nozaki T, Kusuoka O, Omura K, et al. Parp-1 deficiency does not increase the frequency of tumors in the oral cavity and esophagus of ICR/129Sv mice by 4-nitroquinoline 1-oxide, a carcinogen producing bulky adducts. Cancer Lett 2006;241:87–92.
[7] Tseng SH, Yang CC, Yu EH, Chang C, Lee YS, Liu CJ, et al. K14-EGFP-miR-31 transgenic mice have high susceptibility to chemical-induced squamous cell tumorigenesis that is associating with Ku80 repression. Int J Cancer 2015;136:1263–75.
[8] Hawkins BL, Heniford BW, Ackermann DM, Leonberger M, Martinez SA, Hendler FJ. 4NQO carcinogenesis: a mouse model of oral cavity squamous cell carcinoma. Head Neck 1994;16:424–32.
[9] Stenman G. Malignancy of 4NQO-induced oral squamous cell carcinomas in the rat. Acta Otolaryngol 1981;92:557–61.
[10] Li J, Liang F, Yu D, Qing H, Yang Y. Development of a 4-nitroquinoline-1-oxide model of lymph node metastasis in oral squamous cell carcinoma. Oral Oncol 2013;49:299–305.
[11] Kao YY, Tu HF, Kao SY, Chang KW, Lin SC. The increase of oncogenic miRNA expression in tongue carcinogenesis of a mouse model. Oral Oncol 2015;51:1103–12.
[12] Kim TW, Chen Q, Shen X, Regezi JA, Ramos DM, Tanaka H, et al. Oral mucosal carcinogenesis in SENCAR mice. Anticancer Res 2002;22:2733–40.
[13] Eisener-Dorman AF, Lawrence DA, Bolivar VJ. Cautionary insights on knockout mouse studies: the gene or not the gene? Brain Behav Immun 2009;23:318–24.
[14] Chen YF, Yang CC, Kao SY, Liu CJ, Lin SC, Chang KW. MicroRNA-211 enhances the oncogenicity of carcinogen-induced oral carcinoma by repressing TCF12 and increasing antioxidant activity. Cancer Res 2016;76:4872–86.
[15] Chu TH, Yang CC, Liu CJ, Lui MT, Lin SC, Chang KW. miR-211 promotes the progression of head and neck carcinomas by targeting TGFbetaRII. Cancer Lett 2013;337:115–24.
[16] Wei SC, Duffy CR, Allison JP. Fundamental mechanisms of immune checkpoint blockade therapy. Cancer Discov 2018;8:1069–86.
[17] Thomas GR, Chen Z, Oechsli MN, Hendler FJ, Van Waes C. Decreased expression of CD80 is a marker for increased tumorigenicity in a new murine model of oral squamous-cell carcinoma. Int J Cancer 1999;82:377–84.
[18] Judd NP, Winkler AE, Murillo-Sauca O, Brotman JJ, Law JH, Lewis Jr JS, et al. ERK1/2 regulation of CD44 modulates oral cancer aggressiveness. Cancer Res 2012;72:365–74.
[19] Wu YN, Chen DH, Shi XY, Lian CC, Wang TY, Yeh CS, et al. Cancer-cell-specific cytotoxicity of non-oxidized iron elements in iron core-gold shell NPs. Nanomedicine 2011;7:420–7.
[20] Liu CJ, Tsai MM, Hung PS, Kao SY, Liu TY, Wu KJ, et al. miR-31 ablates expression of the HIF regulatory factor FIH to activate the HIF pathway in head and neck carcinoma. Cancer Res 2010;70:1635–44.
[21] Liu CJ, Shen WG, Peng SY, Cheng HW, Kao SY, Lin SC, et al. miR-134 induces oncogenicity and metastasis in head and neck carcinoma through targeting WWOX gene. Int J Cancer 2014;134:811–21.
[22] Peng SY, Tu HF, Yang CC, Wu CH, Liu CJ, Chang KW, et al. miR-134 targets PDCD7 to reduce E-cadherin expression and enhance oral cancer progression. Int J Cancer 2018;143:2892–904.
[23] Chen YF, Wei YY, Yang CC, Liu CJ, Yeh LY, Chou CH, et al. miR-125bsuppresses oral oncogenicity by targeting the anti-oxidative gene PRXL2A. Redox Biol 2019;22:101140.
[24] Kao YY, Chou CH, Yeh LY, Chen YF, Chang KW, Liu CJ, et al. MicroRNA miR-31 targets SIRT3 to disrupt mitochondrial activity and increase oxidative stress in oral carcinoma. Cancer Lett 2019;456:40–8.
[25] Hung PS, Liu CJ, Chou CS, Kao SY, Yang CC, Chang KW, et al. miR-146a enhances the oncogenicity of oral carcinoma by concomitant targeting of the IRAK1, TRAF6 and NUMB genes. PLoS ONE 2013;8. e79926.
[26] Hung PS, Chang KW, Kao SY, Chu TH, Liu CJ, Lin SC. Association between the rs2910164 polymorphism in pre-mir-146a and oral carcinoma progression. Oral Oncol 2012;48:404–8.
[27] Yu EH, Tu HF, Wu CH, Yang CC, Chang KW. MicroRNA-21 promotes perineural invasion and impacts survival in patients with oral carcinoma. J Chin Med Assoc 2017;80:383–8.
[28] Alcoser SY, Kimmel DJ, Borgel SD, Carter JP, Dougherty KM, Hollingshead MG. Real-time PCR-based assay to quantify the relative amount of human and mouse tissue present in tumor xenografts. BMC Biotechnol 2011;11:124.
[29] Chen YF, Liu CJ, Lin LH, Chou CH, Yeh LY, Lin SC, et al. Establishing of mouse oral carcinoma cell lines derived from transgenic mice and their use as syngeneic tumorigenesis models. BMC Cancer 2019;19:281.
[30] Liang S, Peng X, Li X, Yang P, Xie L, Li Y, et al. Silencing of CXCR4 sensitizes triple-negative breast cancer cells to cisplatin. Oncotarget. 2015;6:1020–30.
[31] Li HY, McSharry M, Bullock B, Nguyen TT, Kwak J, Poczobutt JM, et al. The tumor microenvironment regulates sensitivity of murine lung tumors to PD-1/PD-L1 antibody blockade. Cancer Immunol Res 2017;5:767–77.
[32] Kanojia D, Vaidya MM. 4-nitroquinoline-1-oxide induced experimental oral carcinogenesis. Oral Oncol 2006;42:655–67.
[33] Biddle A, Gammon L, Liang X, Costea DE, Mackenzie IC. Phenotypic plasticity determines cancer stem cell therapeutic resistance in oral squamous cell carcinoma. EBioMedicine 2016;4:138–45.